



## Short communication

Electrochemical performance of  $\text{Pr}_{0.7}\text{Sr}_{0.3}\text{Co}_{0.9}\text{Cu}_{0.1}\text{O}_{3-\delta}-\text{Ce}_{0.8}\text{Sm}_{0.2}\text{O}_{1.9}$  composite cathodes in intermediate-temperature solid oxide fuel cells

Chengjun Zhu, Xiaomei Liu\*, Dan Xu, Dejun Wang, Duanting Yan, Li Pei, Tianquan Lü, Wenhui Su

Department of Physics, Jilin University, Changchun 130023, PR China

## ARTICLE INFO

## Article history:

Received 18 April 2008

Received in revised form 11 June 2008

Accepted 11 June 2008

Available online 20 June 2008

## Keywords:

Composite cathode

 $\text{Pr}_{0.7}\text{Sr}_{0.3}\text{Co}_{0.9}\text{Cu}_{0.1}\text{O}_{3-\delta}$ 

Electrochemical performance

SOFC

## ABSTRACT

The electrochemical performance of  $\text{Pr}_{0.7}\text{Sr}_{0.3}\text{Co}_{0.9}\text{Cu}_{0.1}\text{O}_{3-\delta}-x\text{Ce}_{0.8}\text{Sm}_{0.2}\text{O}_{1.9}$  (PSCC- $x$ SDC,  $x=0-40$  wt%) composite cathodes has been investigated for their potential utilization in intermediate-temperature solid oxide fuel cells (SOFCs). The results showed that the addition of SDC to PSCC improved remarkably the electrochemical performance of a PSCC cathode, and that a PSCC-35SDC cathode exhibited the best electrochemical performance in the PSCC- $x$ SDC system. When SDC was used as the electrolyte, the interfacial resistance was smallest for 35 wt% SDC, where the value was  $0.137\ \Omega\ \text{cm}^2$  at  $700\ ^\circ\text{C}$  and  $0.062\ \Omega\ \text{cm}^2$  at  $750\ ^\circ\text{C}$ , much lower than the corresponding interfacial resistance for pure PSCC. At  $700\ ^\circ\text{C}$ , the cathodic overpotential of the PSCC-35SDC cathode in the SDC electrolyte was 70 mV at a current density of  $0.5\ \text{A}\ \text{cm}^{-2}$ . This is a factor of two lower than that for a pure PSCC cathode ( $152\ \text{mV}$  at  $700\ ^\circ\text{C}$ ) under the same current conditions. The maximum power density of a single-cell using PSCC-35SDC as the cathode was 388 and  $615\ \text{mW}\ \text{cm}^{-2}$  at 650 and  $700\ ^\circ\text{C}$ , respectively.

© 2008 Elsevier B.V. All rights reserved.

## 1. Introduction

Solid oxide fuel cells (SOFCs) are considered as one of the most promising energy conversion devices because of their high efficiency, low pollution and flexibility with respect to fuel. However, for traditional SOFC structures, the necessity for high operating temperatures ( $800-1000\ ^\circ\text{C}$ ) has resulted in high costs and material compatibility challenges [1]. As a consequence, significant effort has been devoted to the development of intermediate-temperature ( $500-800\ ^\circ\text{C}$ ) SOFCs [2]. A key obstacle to reduced-temperature operation of SOFCs is the poor activity of traditional cathode materials such as  $\text{La}_{1-x}\text{Sr}_x\text{MnO}_3$  (LSM) for electrochemical reduction of oxygen in this temperature range [1,3]. Accordingly, the development of alternative cathode materials with adequate mixed ionic-electronic conductivity is needed to make intermediate-temperature SOFC technology successful.

Considerable research interest is currently being directed towards cobalt-containing perovskite oxides, which tend to exhibit higher ionic conductivities than LSM owing to a greater concentration of oxygen vacancies [4–6]. Interest has especially grown in Sr-doped  $\text{LaCoO}_3$  (LSC) compositions owing to their high electronic and oxide-ion conductivities [7,8]. Unfortunately, LSC exhibits a

high thermal expansion coefficient due to a low-spin-to-high-spin transition associated with  $\text{Co}^{3+}$ , and high chemical reactivity with the electrolyte [8,9]. These difficulties could be minimized by the replacement of La by other, smaller lanthanides or a partial substitution of Co by other transition metal cations [10,11]. Yasumoto et al. reported that doping with Cu into the Co sites further enhanced the ionic conductivity and catalytic activity of  $(\text{La,Sr})\text{CoO}_{3-\delta}$  [12]. We have recently reported that the composition  $x=0.1$  in the  $\text{Pr}_{0.7}\text{Sr}_{0.3}\text{Co}_{1-y}\text{Cu}_y\text{O}_{3-\delta}$  ( $x=0.05-0.4$ ) system exhibits the best electrochemical performance with adequate electronic conductivity [13].

It is widely accepted that composite cathodes, for example LSM-YSZ or SSC-SDC composite cathodes, can extend the electrochemically active reaction zone from the triple phase boundaries at the two-dimensional interface between the electrolyte and the cathode to the three-dimensional bulk of the electrode, and thus significantly improve the cathode performance [6,14–16]. With the aim of improving the electrocatalytic activity of  $\text{Pr}_{0.7}\text{Sr}_{0.3}\text{Co}_{0.9}\text{Cu}_{0.1}\text{O}_{3-\delta}$  (PSCC) and achieving a match of the thermal expansion coefficient between the electrolyte and the cathode, we present here the electrochemical properties of  $\text{Pr}_{0.7}\text{Sr}_{0.3}\text{Co}_{0.9}\text{Cu}_{0.1}\text{O}_{3-\delta}-\text{Ce}_{0.8}\text{Sm}_{0.2}\text{O}_{1.9}$  composite cathodes. Then, the performance of an anode-supported single-cell using PSCC-35SDC as the cathode, NiO-SDC as the anode and an SDC thin film as the electrolyte is evaluated.

\* Corresponding author. Tel.: +86 431 85172529; fax: +86 431 84638392.  
E-mail address: [xiaomeiliu58@sina.com](mailto:xiaomeiliu58@sina.com) (X. Liu).

## 2. Experimental

A PSCC powder was synthesized by a sol–gel method. Stoichiometric amounts of  $\text{Pr}_6\text{O}_{11}$  (99.99%, Analytical Reagent (A.R.), Shanghai Yuelong New Materials Company Ltd., China),  $\text{Sr}(\text{NO}_3)_2$  (99.5%, A.R., Xinhua Chemical Reagent Plant, Beijing, China),  $\text{Co}(\text{NO}_3)_2 \cdot 6\text{H}_2\text{O}$  (99.9%, A.R., Sinopharm Chemical Reagent Co. Ltd., Shanghai, China) and  $\text{CuO}$  (99.0%, A.R., Shenyang Reagent Plant, Liaoning, China) were used as the starting materials. The  $\text{Pr}_6\text{O}_{11}$  and  $\text{CuO}$  were dissolved completely in concentrated nitric acid (65–68%), and the  $\text{Sr}(\text{NO}_3)_2$  and  $\text{Co}(\text{NO}_3)_2$  were dissolved in distilled water. They were then mixed together to obtain a mixed solution, and citric acid (99.8%, A.R., Beijing Chemical Plant, China) was added as a solid in a molar ratio of 1:1.2 to the metallic ions. The mixed solution was subsequently stirred and heated slowly to form a glutinous colloid. The colloid was dried, ground and calcined at  $800^\circ\text{C}$  for 10 h to obtain the cathode powder.  $\text{ACe}_{0.8}\text{Sm}_{0.2}\text{O}_{1.9}$  (SDC) powder was prepared by the glycine–nitrate process as described elsewhere [17]. Stoichiometric amounts of  $\text{Ce}(\text{NO}_3)_3 \cdot 6\text{H}_2\text{O}$  (99.0%, A.R., Sinopharm Chemical Reagent Co. Ltd., Shanghai, China) and  $\text{Sm}_2\text{O}_3$  (99.99%, A.R., Shanghai Yuelong New Materials Company Ltd., China) were used as the starting materials. The precursor powders were calcined at  $800^\circ\text{C}$  for 2 h to obtain the SDC powder. The SDC powder was cold-pressed into pellets about 13 mm in diameter and 1 mm thick under 360 MPa, and sintered at  $1400^\circ\text{C}$  for 10 h in air to obtain a dense electrolyte substrate.

The PSCC powder obtained was mixed with different amounts of SDC powder (0–40 wt%) to make composite cathodes (denoted here by “PSCC– $x$ SDC”,  $x=0$ –40). The cathode powders were mixed with ethyl cellulose (C.R., Sinopharm Chemical Reagent Co. Ltd., Shanghai, China) and terpineol (A.R., Huadong Chemical Reagent Plant, Tianjin, China) to obtain a well-distributed cathode slurry. The cathode slurry was painted onto one side of the SDC substrate and sintered in air at  $900^\circ\text{C}$  for 2 h. These pellets were used to measure the cathodic overpotential.

In order to evaluate the performance of the cathodes, cells with a structure PSCC–35SDC/SDC/NiO–SDC were fabricated by a dry pressing process. NiO powder was prepared by an ammonia precipitation method as described elsewhere [18]. Ammonia (A.R.) and  $\text{Ni}(\text{NO}_3)_2 \cdot 6\text{H}_2\text{O}$  (A.R., Shantou Xilong Chemical Reagent Plant, Guangdong, China) were used as the starting materials. The NiO and SDC powders obtained were mixed in a weight ratio of 60:40 and ball-milled for 20 h using ethanol as a medium. As a pore former, 15 wt% of flour was added to the mixture, which was subsequently ball-milled for another 2 h. After drying, the anode powder was pressed under 100 MPa into pellets with a diameter of 13 mm to be used as anode substrates. To prepare a thin SDC film on the anode substrate, the prepared SDC powder was added to the anode substrate through a screen (silk net, 180 mesh), and then co-pressed at 220 MPa to obtain a green bilayer. The green bilayer was subsequently sintered at  $1400^\circ\text{C}$  for 4 h to form a dense SDC electrolyte film. A PSCC–35SDC powder was mixed with ethyl cellulose and terpineol, painted onto the sintered SDC film and sintered in air at  $900^\circ\text{C}$  for 2 h. Silver paste was applied to the anode and cathode surfaces to serve as current collectors, followed by attachment of two silver wires to each electrode to serve as current and voltage leads. The single-cell made in this way was then sealed onto one end of an alumina tube with silver paste. The performance of the cell was tested from  $600$  to  $700^\circ\text{C}$ . Hydrogen was used as the fuel at the anode side, and air as the oxidant at the cathode side.

The crystal structure and phase purity were characterized by X-ray diffraction (XRD) (Rigaku-D-Max Ra system,  $\text{Cu K}\alpha$  radiation, operated at 12 kW). The cathodic overpotential was measured in air with a Solartron SI 1287 electrochemical interface-measuring apparatus using a current-interruption technique. Interfacial polar-

ization resistances were determined on symmetric cells with a two-electrode configuration using AC impedance spectroscopy (CHI 604C, Chenhua Inc., Shanghai). The frequency range was  $0.01$ – $10^5$  Hz with a signal amplitude of 10 mV. The morphologies of the cathodes after the electrochemical tests were characterized by a scanning electron microscope (SEM, JSM-6480LV, JEOL, Japan). The single-cell performance was tested at temperatures from  $600$  to  $700^\circ\text{C}$ .

## 3. Results and discussion

Fig. 1 shows an XRD pattern of a PSCC–35SDC composite cathode. For comparison, the patterns of PSCC and SDC are also shown in the same figure. It can be seen that the PSCC cathode material synthesized by the sol–gel method is single-phase with an orthorhombic perovskite structure. The structure of the SDC is the cubic fluorite structure. After the PSCC–35SDC mixture has been sintered at  $900^\circ\text{C}$  for 8 h, the PSCC and SDC still retain their own structures. This suggests that there are no obvious reactions between PSCC and SDC or solid solution formation. It seems that PSCC is a chemically stable cathode material for SOFCs based on SDC when the operating temperature is below  $900^\circ\text{C}$ .

Fig. 2 shows cathodic polarization curves for PSCC and PSCC–SDC composite cathodes as a function of current density at  $650$  and  $700^\circ\text{C}$  in air. It is very clear that the addition of the SDC electrolyte to the PSCC leads to a remarkable improvement in electrode performance. At each temperature, the overpotential for these two-phase composite cathodes decreases with increasing SDC content  $x$  for  $0 \leq x \leq 0.35$ , reaches a minimum at  $x=0.35$ , and then increases for  $x=0.4$ . At  $700^\circ\text{C}$ , the overpotential for the pure PSCC is  $152$  mV at  $0.5$   $\text{A cm}^{-2}$ . For the PSCC–35SDC cathode, the overpotential is reduced to  $70$  mV under the same current conditions. Similar improvements in the electrode polarization performance are also observed at  $650^\circ\text{C}$ .

The cathode performance of the PSCC and PSCC–SDC sintered at  $900^\circ\text{C}$  for 2 h was investigated by AC impedance spectroscopy based on a symmetric cell configuration under a symmetric air atmosphere. The impedance curves were measured under open-circuit conditions. Nyquist plots of the electrochemical impedance spectra for PSCC and PSCC–SDC at  $700^\circ\text{C}$  are shown in Fig. 3(a), and the equivalent circuit for the analysis of the impedance data

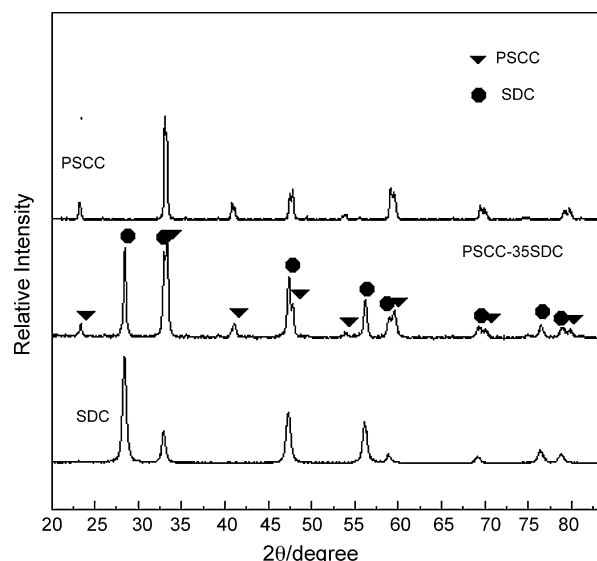


Fig. 1. XRD patterns of PSCC, SDC and PSCC–35SDC.

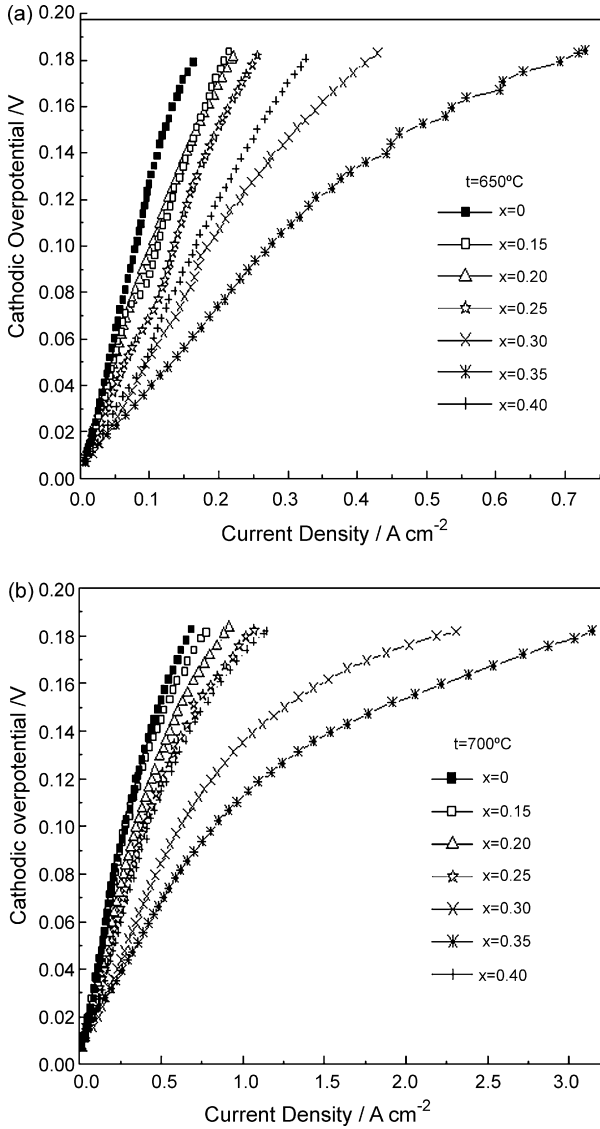


Fig. 2. Overpotential curves for PSCC-xSDC composites obtained at 650 and 700 °C.

is illustrated in Fig. 3(b). The impedance spectra consist of two depressed semicircles. This indicates that there are at least two-electrode processes, corresponding to the two semicircles, during reduction of molecular oxygen. As discussed by previous workers [19,20], the high-frequency semicircle can be attributed to polarization during charge transfer. The low-frequency semicircle can be attributed to oxygen adsorption/dissociation on the electrode surface and diffusion of the oxygen ions. The elements of the equivalent circuit correspond to elements of the electrochemical process.  $R_1$  corresponds to the resistance of the ohmic polarization,  $R_2$  corresponds to the resistance of the charge transfer process through the electrode-electrolyte interface, and the Warburg impedance ( $W_1$ ) in the equivalent circuit is related to the resistance of oxygen adsorption/decomposition and the diffusion of oxygen ions in the cathode [21];  $CPE_1$  corresponds to the capacitance of the whole electrode.

Fig. 4 summarizes the total interfacial polarization resistance  $R_p$  (i.e., the difference between the intercepts of the impedance arc on the real axis) for each of the PSCC-SDC cathodes tested in air. It can be seen that  $R_p$  decreases as the SDC concentration increases up to 35 wt%. A further increase in SDC content to a

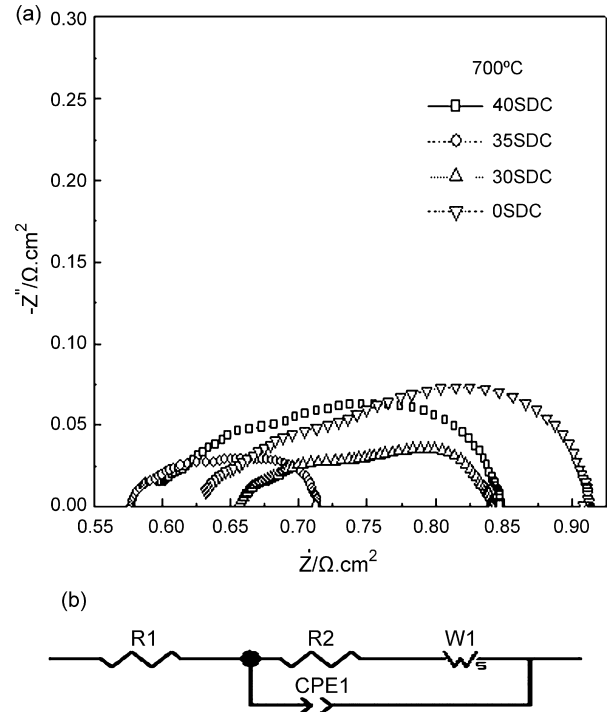


Fig. 3. (a) Impedance spectra of the PSCC cathode and PSCC-SDC composite cathode at 700 °C and (b) equivalent circuit.

value higher than 35 wt% results in a higher interfacial polarization resistance. This may be due to a decrease in the continuity of the PSCC phase in the composite, and hence a decrease in electrical conductivity [15]. This corresponds very well to the results for the overpotential (Fig. 2). The interfacial resistance  $R_p$  was about  $0.282 \Omega \text{ cm}^2$  at 700 °C for pure PSCC. However, the optimal composition, PSCC-35SDC, yielded an  $R_p$  value of less than  $0.137 \Omega \text{ cm}^2$  at 700 °C. Thus the addition of SDC could dramatically improve the electrochemical performance of PSCC.  $\text{CeO}_2$ -based oxides are known for their ability to store, release and transport oxygen under SOFC operating conditions owing to their high ionic conductivity [22]. The oxygen ion conductivity of  $\text{Sm}_{0.2}\text{Ce}_{0.8}\text{O}_{1.9}$  has been

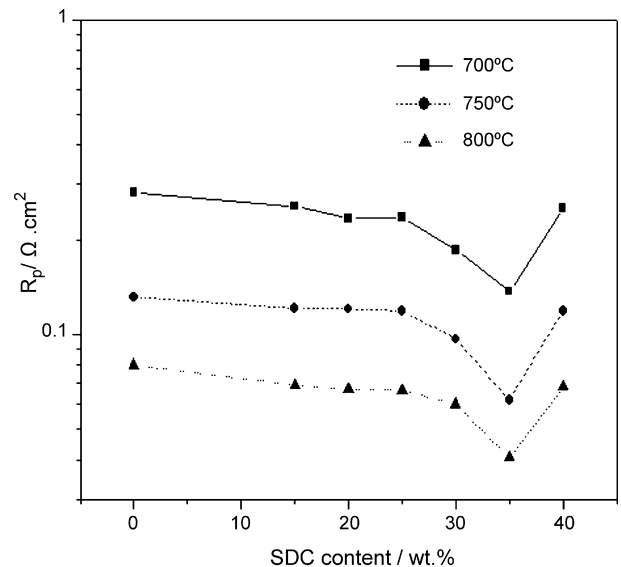


Fig. 4. Total interfacial resistance versus cathode composition at 700–800 °C.



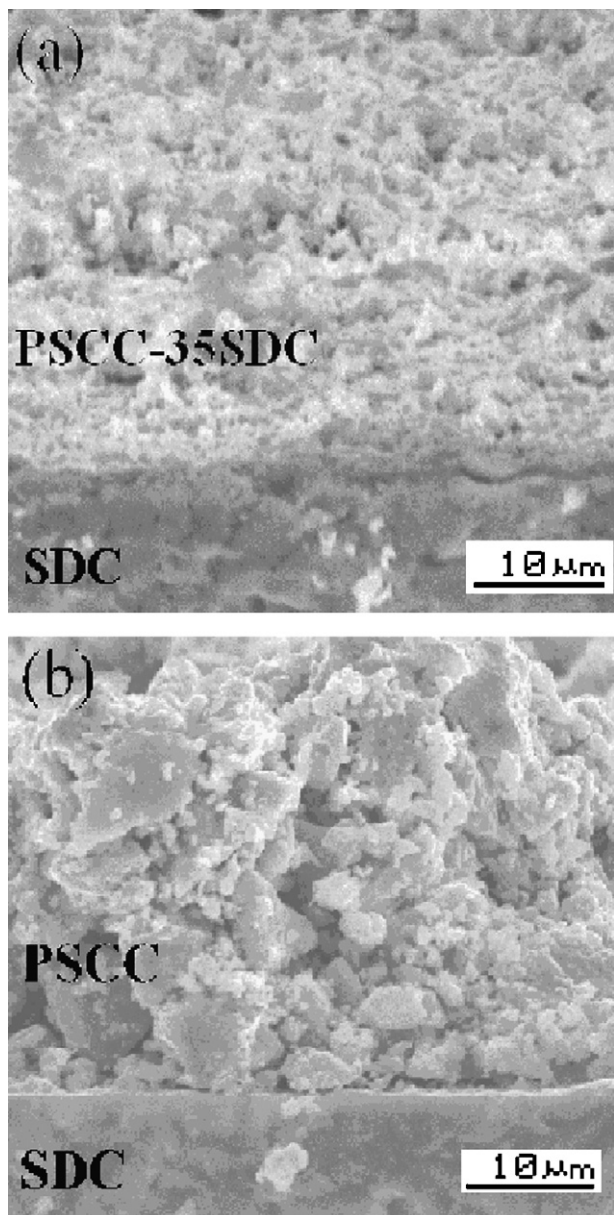


Fig. 5. SEM cross-sectional images of half-cells with (a) a PSCC–35SDC composite cathode and (b) a PSCC cathode layer, after electrochemical tests.

reported to be as high as  $0.084 \text{ S cm}^{-1}$  at  $800^\circ\text{C}$  [23]. This indicates that the ionically conducting phase SDC, when added to a porous cathode, functions effectively as an oxygen conduction path, greatly extending the electrochemically active reaction sites from the electrode/electrolyte interface region to the bulk of the PSCC electrode. This reduces the resistance of charge transfer  $R_2$ . At the same time, the addition of this ionically conducting phase also increases the total concentration of oxygen vacancies and the diffusion of oxygen ions in the electrode is improved, which results in a decrease in the Warburg resistance  $W_1$ . Therefore, a decrease in the total interfacial polarization resistance  $R_p$  owing to the addition of SDC can be expected.

It is well known that the microstructure of a cathode can have a significant effect on cathode performance. Micrographs of cross-sectional views of PSCC–35SDC/SDC and PSCC/SDC half-cells after electrochemical tests are shown in Fig. 5(a) and (b), respectively. It is evident that the PSCC–35SDC composite cathode has a smaller

grain size and a more homogeneous grain size distribution. This means that the PSCC–35SDC cathode layer has a finer microstructure than the pure PSCC cathode layer has. Moreover, the visual appearance of the electrolyte/cathode interface in the micrographs indicates clearly that the porous PSCC–35SDC composite cathode shows better adhesion to the dense SDC than does the pure PSCC cathode. Adding SDC particles to PSCC has two functions: on the one hand, it helps to reduce the thermal expansion coefficient of the cathode and thus makes it mechanically more compatible with the electrolyte; on the other hand, it also results in suppression of the growth of PSCC particles, thereby maintaining the porosity, optimizing the connectivity between the particles of each solid phase and optimizing the size distribution, so as to yield a larger three-phase (cathode–electrolyte–gas) contact area that is accessible for oxygen reduction [16]. This partly explains why the PSCC–35SDC composite cathode exhibited a higher electrochemical performance in general compared with the pure PSCC cathode.

Fig. 6 shows plots of the performance of a single fuel cell with PSCC–35SDC as the cathode and NiO/SDC as the anode and with an SDC electrolyte film, at  $600$ – $700^\circ\text{C}$ . It can be seen that the power density and current density increase with increasing operating temperature. The maximum power density of the cell is  $204$ ,  $388$  and  $615 \text{ mW cm}^{-2}$  at  $600$ ,  $650$  and  $700^\circ\text{C}$ , respectively, illustrating that good performance can be obtained for a single fuel cell using PSCC–35SDC as the cathode and an SDC film as the electrolyte. However, the open-circuit voltage (OCV) of this cell based on an SDC membrane is relatively low, about  $0.685 \text{ V}$  at  $650^\circ\text{C}$ , which is much lower than the theoretical OCV [24]. According to the report of Zhang et al. [25], a thinner electrolyte film not only will reduce the cell resistance, but also will enhance the possibility of defects in the electrolyte such as pinholes or microcracks spanning the entire electrolyte thickness, leading to a lower OCV because of gas leakage.

AC impedance spectra of the cell under open-circuit conditions are plotted in Fig. 7. The high-frequency intercept with the real axis gives the ohmic losses ( $R_o$ ), and the difference between the high-frequency and low-frequency intercepts represents the sum of the electrode interfacial resistances in the cell. The electrode interfacial resistance ( $R_e$ ), which is higher than the ohmic resistance (Table 1), accounts for about  $54.7$ – $64.8\%$  of the total cell resistance ( $R_t$ ) from  $600$  to  $700^\circ\text{C}$ . This implies that the performance of the cell is critically limited by the interfacial resistance. According to previous studies [26,27], the interfacial resistance is dominated by the cathode–electrolyte interface, and the resistance

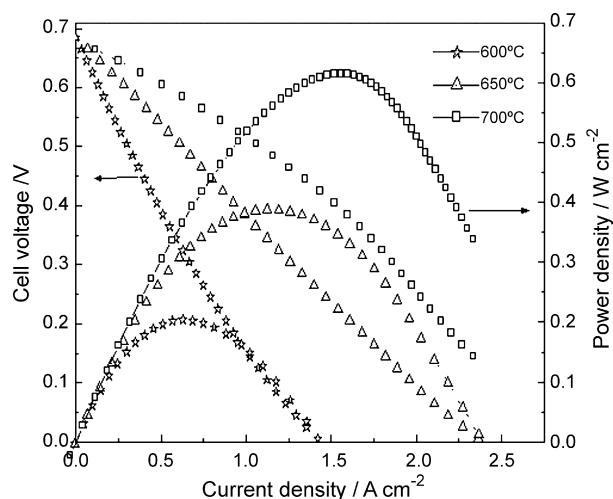


Fig. 6. Performance of a cell with a PSCC–35SDC composite cathode at  $600$ – $700^\circ\text{C}$ . Hydrogen and ambient air were used as the fuel and oxidant, respectively.

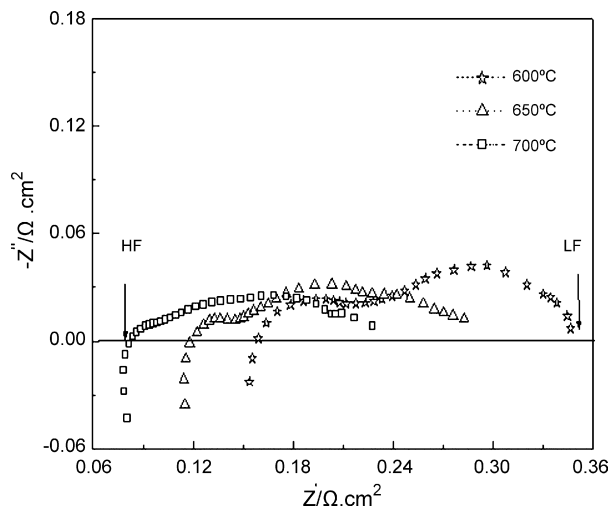


Fig. 7. Impedance spectra of a single-cell (PSCC-35SDC/SDC/NiO-SDC) measured under open-circuit conditions (HF, high frequency; LF, low frequency).

Table 1

Ohmic polarization resistance ( $R_o$ ), electrode interfacial resistance ( $R_e$ ) and total cell resistance ( $R_t$ ) for a single PSCC-35SDC/SDC/NiO-SDC cell at different operating temperatures

Temperature ( $^{\circ}\text{C}$ )	$R_o$ ( $\Omega \text{ cm}^2$ )	$R_e$ ( $\Omega \text{ cm}^2$ )	$R_t$ ( $\Omega \text{ cm}^2$ )	$R_e/R_t$ (%)
600	0.158	0.191	0.349	54.7
650	0.118	0.178	0.296	60.1
700	0.083	0.153	0.236	64.8

of the anode–electrolyte interface is negligible. Therefore reducing the cathode–electrolyte interfacial resistance is the key to reducing the total resistance as well as to improving the performance of the cell.

#### 4. Conclusions

A new PSCC-SDC composite cathode for potential application in intermediate-temperature SOFCs has been reported. The addition of an SDC electrolyte to the PSCC greatly improved the electrochemical performance of the PSCC cathode. A PSCC cathode containing 35 wt% SDC exhibited a low overpotential. The interfacial polarization resistance for this PSCC-35SDC cathode was as low as  $0.062 \Omega \text{ cm}^2$  at  $750^{\circ}\text{C}$  and  $0.137 \Omega \text{ cm}^2$  at  $700^{\circ}\text{C}$ . Using a PSCC-35SDC cathode, an anode-supported single-cell

with an SDC electrolyte membrane achieved excellent performance. The maximum power density of this cell was 204, 388 and  $615 \text{ mW cm}^{-2}$  at 600, 650 and  $700^{\circ}\text{C}$ , respectively. These results indicate that PSCC-35SDC should be a good candidate for intermediate-temperature SOFC cathode materials.

#### Acknowledgments

This work was supported by a project supported by the National Natural Science Foundation, China, under contract no. 10674034, and also the National Fund for Fostering Talent in Basic Science, China, under contract no. J0730311.

#### References

- [1] N.P. Brandon, S. Skinner, B.C.H. Steele, *Ann. Rev. Mater. Res.* 33 (2003) 183–213.
- [2] N.Q. Minh, *J. Am. Ceram. Soc.* 76 (1993) 563–588.
- [3] M.T. Colomer, B.C.H. Steele, J.A. Kilner, *Solid State Ionics* 147 (2002) 41–48.
- [4] R.A. De Souza, J.A. Kilner, *Solid State Ionics* 106 (1998) 175–187.
- [5] E. Maguire, B. Gharbage, F.M.B. Marque, J.A. Labrincha, *Solid State Ionics* 127 (2000) 329–335.
- [6] V. Dusastre, J.A. Kilner, *Solid State Ionics* 126 (1999) 163–174.
- [7] A.N. Petrov, O.F. Kononchuk, A.V. Andreev, V.A. Cherepanov, P. Kofstad, *Solid State Ionics* 80 (1995) 189–199.
- [8] O. Yamamoto, Y. Takeda, R. Kanno, N. Noda, *Solid State Ionics* 22 (1987) 241–246.
- [9] L.W. Tai, M.M. Nastrallah, H.U. Anderson, D.M. Sparlin, S.R. Sehlin, *Solid State Ionics* 76 (1995) 259–271.
- [10] K.T. Lee, A. Manthiram, *J. Electrochem. Soc.* 153 (2006) A794–A798.
- [11] K.T. Lee, A. Manthiram, *Solid State Ionics* 178 (2007) 995–1000.
- [12] K. Yasumoto, Y. Inagaki, M. Shiono, M. Dokiya, *Solid State Ionics* 148 (2002) 545–549.
- [13] C.J. Zhu, X.M. Liu, D. Xu, D.T. Yan, D.Y. Wang, W.H. Su, *Solid State Ionics* (2008), doi:10.1016/j.ssi.2008.01.031.
- [14] M.J. Jorgensen, S. Primdahl, M. Mogensen, *Electrochim. Acta* 44 (1999) 4195–4201.
- [15] E.P. Murray, S.A. Barnett, *Solid State Ionics* 143 (2001) 265–273.
- [16] C.R. Xia, W. Rauch, F.L. Chen, M.L. Liu, *Solid State Ionics* 149 (2002) 11–19.
- [17] D. Xu, X.M. Liu, D.J. Wang, G.Y. Yi, Y. Gao, D.S. Zhang, W.H. Su, *J. Alloys Compd.* 429 (2007) 292–295.
- [18] Y.H. Zhang, X.Q. Huang, Z. Lü, Z.G. Liu, X.D. Ge, J.H. Xu, X.S. Xin, X.Q. Sha, W.H. Su, *J. Power Sources* 160 (2006) 1217–1220.
- [19] F.H. Henuveln, H.J.M. Bouwmeester, *J. Electrochem. Soc.* 144 (1997) 134–137.
- [20] Y.J. Leng, S.H. Chan, K.S. Khor, S.P. Jiang, *Int. J. Hydrogen Energy* 29 (2004) 1025–1033.
- [21] H.C. Yu, F. Zhao, A.V. Virkar, K.Z. Fung, *J. Power Sources* 152 (2005) 22–26.
- [22] M. Mogensen, N.M. Sammes, G.A. Tompsentt, *Solid State Ionics* 129 (2000) 63–94.
- [23] S.W. Zha, C.R. Xia, G.Y. Meng, *J. Power Sources* 115 (2003) 44–48.
- [24] T. Matsui, T. Kosaka, M. Inaba, A. Mineshige, Z. Ogumi, *Solid State Ionics* 176 (2005) 663–668.
- [25] X.G. Zhang, M. Robertson, C. Deces-Petit, W. Qu, O. Kesler, R. Maric, D. Ghosh, *J. Power Sources* 164 (2007) 668–677.
- [26] S. De Souza, S.J. Visco, L.C. De Jonghe, *J. Electrochem. Soc.* 144 (1997) L35–L37.
- [27] C.R. Xia, M.L. Liu, *Solid State Ionics* 152–153 (2002) 423–430.